Research Article

Characteristic of the cellular spectrum of lymphocyte and macrophage populations in the fibrous capsule and pericystic pulmonary tissue in pulmonary hydatid cyst in children

Babuci S.,[1, 3] **Petrovici V.,**[2] **Dogotari N.,**[1] **David V.**[2]

[1]*PHI Institute of Mother and Child, Natalia Gheorghiu National Scientific and Practical Center of Pediatric Surgery*
[2]*Department of clinical morphopathology*
[3]*Laboratory of surgical infections in children of NicolaeTestemitanu SUMPh*[1]

Abstract

Caracteristica spectrului celular al populaţiei limfocitare şi a macrofagelor în capsula fibroasă şi ţesutul pulmonar perichistic în chistul hidatic pulmonar la copii

În cazurile de chist hidatic relația gazdă-parazit este interactivă, evoluția bolii fiind dependentă de echilibrul între mecanismele sistemului imun ale gazdei și de strategiile complexe de evaziune ale agentului parazitar.
Scopul studiului a fost testarea imunohistochimică a populației limfocitare în componența infiltratului inflamator la nivelul stratului adventicial (perichist) și țesuturile perichistice în diferite forme clinico-morfologice ale chistului hidatic pulmonar la copii.
Investigaţiile morfopatologice au fost direcționate în testarea imunohistochimică a tipurilor de limfocite T implicate în imunitatea celulară locală, cât şi aprecierea limfocitelor B și a macrofagilor implicate în componenta celulară inflamatorie cu utilizarea anticorpilor monoclonali împotriva markerilor de suprafață CD3, CD4, CD8, CD20cy-pozitive și CD68. În calitate de material de studiu au servit probele tisulare prelevate intraoperator din capsula fibroasă și țesuturile adiacente la 20 pacienți cu hidatidoză pulmonară cu vârsta între 10-16 ani, grupați în 3 loturi: 1) chist hidatic pulmonar necomplicat (7 copii); 2) chist hidatic pulmonar cu semne de inflamație ăperichistică (7 copii) și 3) chist hidatic pulmonar complicat prin ruptură (6 copii).
Rezultatele studiului au permis de a conchide că:

1. Evoluția chistului hidatic pulmonar la copii este caracterizată de un infiltrat inflamator cronic al parenchimului perichistic cu predominarea limfocitelor T CD3 comparativ cu capsula fibroasă, unde predomină procesele necrolitice.
2. Numărul sporit de CD20 indică activarea semnificativă a sistemului imun adaptativ în agravarea proceselor inflamatorii în parenchimul perichistic în formele complicate ale maladiei, creșterea numărului de macrofage în aceste cazuri fiind nesemnificativă.
3. Numărul de macrofage CD68 din capsula fibroasă și la nivelul pleurei a fost semnificativ mai mic comparativ cu densitatea acestor celule depistate în infiltratele inflamatorii din parenchimul pulmonar subiacent capsulei fibroase, un număr nesemnificativ mai mare fiind constatat în formele complicate ale maladiei.

Cuvinte cheie: chist hidatic, hidatidoză pulmonară, process inflamator local

Abstract

In cases of hydatid cyst the host-parasite relationship is interactive, the evolution of the disease being dependent on the balance between the mechanisms of the host immune system and complex escape strategies of the parasitic agent.

The *purpose* of the study was to carry out the immunohistochemical test of the lymphocyte population in the inflammatory infiltration at the adventitial layer (pericyst) and pericystic tissues in different clinico-morphological forms of the pulmonary hydatid cyst in children.

Morphopathological investigations were focused on the immunohistochemical testing of T lymphocytes involved in local cell immunity, as well as the assessment of B lymphocytes and macrophages involved in the inflammatory cell component with the use of monoclonal antibodies against surface markers CD3, CD4, CD8, CD20cy-positive and CD68. As a study material, the tissue samples taken intraoperatively from the fibrous capsule and adjacent tissues in 20 patients with pulmonary hydatidosis, aged 10-16 year,s were grouped into 3 groups: 1) uncomplicated pulmonary hydatid cyst (7 children); 2) pulmonary hydatid cyst with signs of pericystic inflammation (7 children), and 3) pulmonary hydatid cyst complicated by rupture (6 children).

The results of the study allowed us to conclude that:

1. The evolution of the pulmonary hydatid cyst in children is characterized by a chronic inflammatory infiltration of the pericystic parenchyma with the predominance of CD3 T lymphocytes compared to the fibrous capsule where the necrolytic processes predominate.
2. The increased number of CD20 indicates a significant activation of the adaptive immune system in the aggravation of inflammatory processes in the pericystic parenchyma in complicated forms of the disease, the increase of the number of macrophages in these cases being insignificant.
3. The number of CD68 macrophages in the fibrous capsule and within the pleura was significantly lower compared to the density of these cells detected in inflammatory infiltrates of the pulmonary parenchyma underlying the fibrous capsule, an insignificant number being found in complicated forms of the disease.

Keywords: gastroschisis, omphalocele, newborn, associated congenital malformations, prognosis

Correspondence to: E-mail: nicolae-dogotari@mail.ru; mob. +37367156999

Introduction

The hydatid cyst represents an endemic zoonotic parasitic disease caused by the *Echinococcus granulosus* metacestode (larval stage), in which the human is an accidental intermediate host, the disease being characterized by cystic lesions occurring in different organs and tissues, most commonly affecting the liver and lung [12, 26, 33]. Morphologically, the hydatid larval cyst is composed of three structural components: the acellular laminar membrane, germinal membrane and hydatid fluid with germinal elements, the metacestode being surrounded by a fibrous capsule (pericyst) or granulation tissue, including inflammatory infiltrates [6, 21]. The pericyst, also called the adventitial layer, is the outer zone of the hydatid cyst, which develops through the reaction of the host tissue to the parasite and consists almost entirely of host cells [10, 25].

In cases of hydatid cyst the host-parasite relationship is interactive, the evolution of the disease being dependent on the balance between the mechanisms of the host immune system and complex escape strategies of the parasitic agent [37], which include antigenic variation, suppression and modulation of T cells, inhibition of chemotaxis of effector cell, release of antigenic proteins, antioxidant defense, resistance to host proteolytic enzymes, etc. Understanding these biological events is of fundamental importance in defining the diagnosis and treatment tactics [19, 27, 39]. It is known that the infection induces an immune imbalance on the tissues of the affected organ with a severe destruction of the architecture, caused by inflammatory infiltrates and the development of fibrosis. This process is caused by the persistent activation of the immune system, which imposes unfavorable changes on normal homeostasis of the organ, at the same time the parasite evading the defense forces of the host organism with the subsequent chronicization of the infection. In this context, the developmental aspects of local immune responses in organs affected by the hydatid cyst remain largely unknown [34].

The marked and persistent antigenic action of this parasitic agent is characterized by a major potential causing an inflammatory reaction, the local reaction being quite varied from severe granulomatous changes, associated with cysts degeneration and their eventual death, up to a collagen capsule, derived from the inflammation resolution correlated with a stable host-parasite relationship, the particularities of inflammatory reactions in pericystic tissues being determinant in the pathogenesis, clinical evolution and development of complications of the disease [7]. The control of *E. granulosus* infection is a complex process, involving the humoral and cellular components of the immune system, the immune defense reactions against an extracellular pathogen being dependent on the interaction of macrophages with T lymphocytes [5, 39].

T lymphocytes are an important type of immunocompetent cells that can produce a series of

morphological and functional changes. These cells and their subtypes have mutual coordination and antagonism during an *in vivo* immune response to maintain balance. The assessment of T lymphocytes, especially the balance of CD4 and CD8 subtypes, has a central position in the evaluation of cellular immunity and the role of these cells in neutralizing the hydatid infection [39]. According to some studies, parasite-derived substances regulate the host immune response by inducing protection (Th1 expansion) or susceptibility to disease (Th2 expansion) [18, 23, 27]. The production of Th1-polarized cytokine in early stages can kill the metacestode in the early stages of development, subsequently passing to a response with Th2 cytokine predominance characteristic for the chronic stage of *E.granulosus* infection, considering that Th2 cytokines are responsible for the inhibition of parasite destruction due to the anti-inflammatory action of IL-10 [40].

Th2 cells express IL-4, IL-5, IL-6 and IL-10, in which Th1 cells probe IL-2 and IFN-γ, accepting the fact that Th2 cytokines participate in the regulation of Th1-derived cytokines and vice versa. It has been shown that in human hydatid disease these cytokines coexist, the Th2 response benefiting the parasite, and the Th1 response benefiting the host [2].

There are many studies that have reported the results of immunity indices changes in circulating blood in cases of human hydatidosis [13, 23], but few data on the local immune response are described, most of the studies being carried out in the hepatic forms of the parasitic disease [35] or in animals [38].

The *purpose* of the study was to carry out the immunohistochemical test of the lymphocyte population in the inflammatory infiltration at the adventitial layer (pericyst) and pericystic tissues in different clinico-morphological forms of the pulmonary hydatid cyst in children.

Material and Methods

Morphopathological investigations were focused on the immunohistochemical testing of T lymphocytes involved in local cell immunity, as well as the assessment of B lymphocytes and macrophages involved in the inflammatory cell component with the use of monoclonal antibodies against surface markers CD3, CD4, CD8, CD20cy-positive and CD68 (table 1). As a study material, the tissue samples taken intraoperatively from the fibrous capsule and adjacent tissues in 20 patients with pulmonary hydatidosis, aged 10-16 year,s were grouped into 3 groups: 1) uncomplicated pulmonary hydatid cyst (7 children); 2) pulmonary hydatid cyst with signs of pericystic inflammation (7 children), and 3) pulmonary hydatid cyst complicated by rupture (6 children).

After preventive fixation of tissue samples in buffered formalin solution (pH =7.2-7.4) for 19-22 hours, they were processed according to the standard protocol for immunohistochemical examination, carried out in accordance with a special methodology. Sections subjected to immunohistochemical staining were subjected to deparaffinization. In order to facilitate labeling of the desired antigen with a specific antibody, deparaffinization is an essential primary step in immunohistochemical method.

***Table 1.* Immunohistochemical methods used in the study**

Antibody	Clone	Manufacturer	Dilution	System	Incubation time	Antigen unmasking
CD3	Monoclonal mouse	DakoCytomation	1:100	EnVision™ FLEX	30 min	Water bath with Target Retrieval high pH, 20 min
CD4	FLEX Monoclonal mouse 4B12	DakoCytomation	RTU	EnVision™ FLEX	15 min	Water bath with Target Retrieval high pH, 20 min
CD8	FLEX Monoclonal mouse C8/144B	DakoCytomation	RTU	EnVision™ FLEX	15 min	Water bath with Target Retrieval high pH, 20 min
CD20cy	FLEX Monoclonal mouse L26	DakoCytomation	1:2	EnVision™ FLEX	15 min	Water bath with Target Retrieval high pH, 20 min
CD68	FLEX Monoclonal mouse PG-M1	DakoCytomation	RTU	EnVision™ FLEX	15 min	Water bath with Target Retrieval high pH, 20 min

It has been shown that the action of organic solvent at 57° C results in a more effective dilution of the inclusion material. For this, the histological slides were subject to 2 toluene baths. The first bath lasted 60 min. in the thermostat at 59° C. The next bath was carried out at room temperature for 5 min. After deparaffining, the solvent was removed by placing it in successive baths of toluene + ethyl alcohol in the ratio of 1:1 for 5 minutes, 96% ethyl alcohol in two sessions, each stage lasted 5 minutes and two washing sessions with distilled water for 10-15 minutes each. Subsequently, the preparations were subjected to antigen unmasking, in order to break disulfide bonds and to expose antigenic epitopes more accessible to the primary antibody. Antigen unmasking was performed by heating it in a hot water bath, the histological slides being included in a helindal, where the temperature of the high pH Target Retrieval (Dako Cytomation Denmark) unmasking solution reached 95-96°C, the unmasking time being 20 min, with an additional pre- and post-treatment time of 60 min. After unmasking, the preparations were washed in diluted Wash buffer (1:20 distilled water) from the kit for 5 min., removing the excess buffer from the blade edge. After this stage the immunohistochemical process itself began. In the researches carried out, the manual IHC method was used along with the standardized EnVision^{TM} FLEX visualization system in the laboratory. After removing the excess buffer from the slide edge, the primary antibody was applied with individual incubation time for each (table). When the exposure time expired, the antibody was washed in two sessions with Wash Buffer for 5 minutes, removing the excess of washing solution. To block endogenous peroxidase, the slides were processed with undiluted peroxidase from the kit for 5 minutes, then washed in distilled water and Wash buffer successively for 5 minutes. Subsequently, the secondary antibody (HRP) was applied for 20 min. with the subsequent washing in two Wash Buffer sessions for 5 minutes each. After the excess buffer was removed, chromogen 3',3-diaminobezidine (DAB, Dako Cytomation Denmark) was applied for 3 min. in order to identify by color reaction (brown) the localization of antibodies chains. After 3 minutes, the excess DAB was removed with distilled water in two sessions for 5 minutes each. Hematoxylin was used to carry out contrasting for 1.5 min. with the subsequent washing in tap water. Subsequently, the preparations were subjected to 2 successive 96% alcohol baths, alcohol + toluene bath (1:1 ratio), two toluene baths for 5 minutes for all baths and the last toluene bath for 10 min. for final clarifying, followed by fixation in Canada balm. The method described above was applied in the case of simple immunolabeling (application of a single primary antibody). The cell density was found in 5 different visual fields in 5 different sections in a patient.

Results. The results of the study allowed us to find that in group 1 the inflammatory infiltrates of the pericystic pulmonary parenchyma underlying the fibrous capsule are dominated by $CD3^+$ lymphocytes ($p<0.01$), T lymphocytes practically missing in the fibrous capsule. The density of $CD3^+$ lymphocytes constituted 239.8$\pm$ 29.7 cells in the visual field, these being dispersed scatteredly and in agglomerations of cellular micropseudonodules (fig. 1A), also forming perivascular agglomerations in the perivascular inflammatory infiltrate (fig. 1B). The number of $CD4^+$ subpopulations in the inflammatory infiltrate of the pericystic pulmonary parenchyma was comparatively smaller (114.0$\pm$11.3 cells/field), being spread in pseudofollicular (fig. 1C) or discretely disperse (fig. 1D) appearance. The density of $CD8^+$ subpopulation was lower (126.8 $\pm$ 4.1 cells/field) compared to the density of $CD3^+$ cells ($p <0.01$), insignificantly exceeding the density of $CD4^+$ cells ($p>0.05$), these cells being widespread in dispersed appearance (fig. 1E, F). In group 1, B lymphocytes, identified by $CD20^+$ expression, were present in a number of 128.00 $\pm$ 14.2 cells/field, usually being located in the inflammatory infiltrate of the pulmonary parenchyma underlying the fibrous capsule, having lymphocyte infiltrate appearance in plates, pseudofollicularly and dispersedly, these cells missing in the fibrous capsule (fig. 2). The density of CD68 cells in the parenchyma adjacent to the fibrous capsule was quite high (189$\pm$13.4 cells/field) (fig. 3A), these cells being observed in perivascular infiltrates (fig. 3B), and in a quite large number within the fibrous capsule limits (fig. 3C) and regional pleura (fig. 3D).

In study group 2, the density of $CD3^+$ lymphocytes from the inflammatory infiltrate in the parenchyma adjacent to the fibrous capsule (257.25 $\pm$ 54.7 cells/field) significantly exceeded the values of $CD4^+$ and $CD8^+$ subpopulations ($p>0.05$), without finding a veridical difference compared with study group 1 ($p>0.05$). In these cases, $CD3^+$ lymphocytes were diffusely dispersed in the pericystic parenchyma, a higher density being determined in peribronchial spaces, single cells being observed in the fibrous capsule area (fig. 4A, B). In this group of patients $CD4^+$ subpopulation had a higher density (228.5$\pm$34.8 cells/field) compared to the values of group 1 ($p<0.01$), these cells being spread as pseudofollicular structures, located closely to the fibrous capsule (fig. 4C), these structures being well expressed in peribronchial spaces (fig. 4D). The density values of $CD8^+$ subpopulation (171$\pm$16.4 cells/field) exceeded statistically veridically values found in study group 1 ($p<0.05$), the cells of this subpopulation being spread irregularly. There were sectors with subpopulation density of 267 cells in the field of view, while in other areas - only 51 cells. Usually, $CD8^+$ cells were observed around the fibrous capsule in the form of pseudofollicular structures, these structures being also found peribronchially (fig. 4E), while in the distant interstice these cells were dispersely spread (fig. 4F).

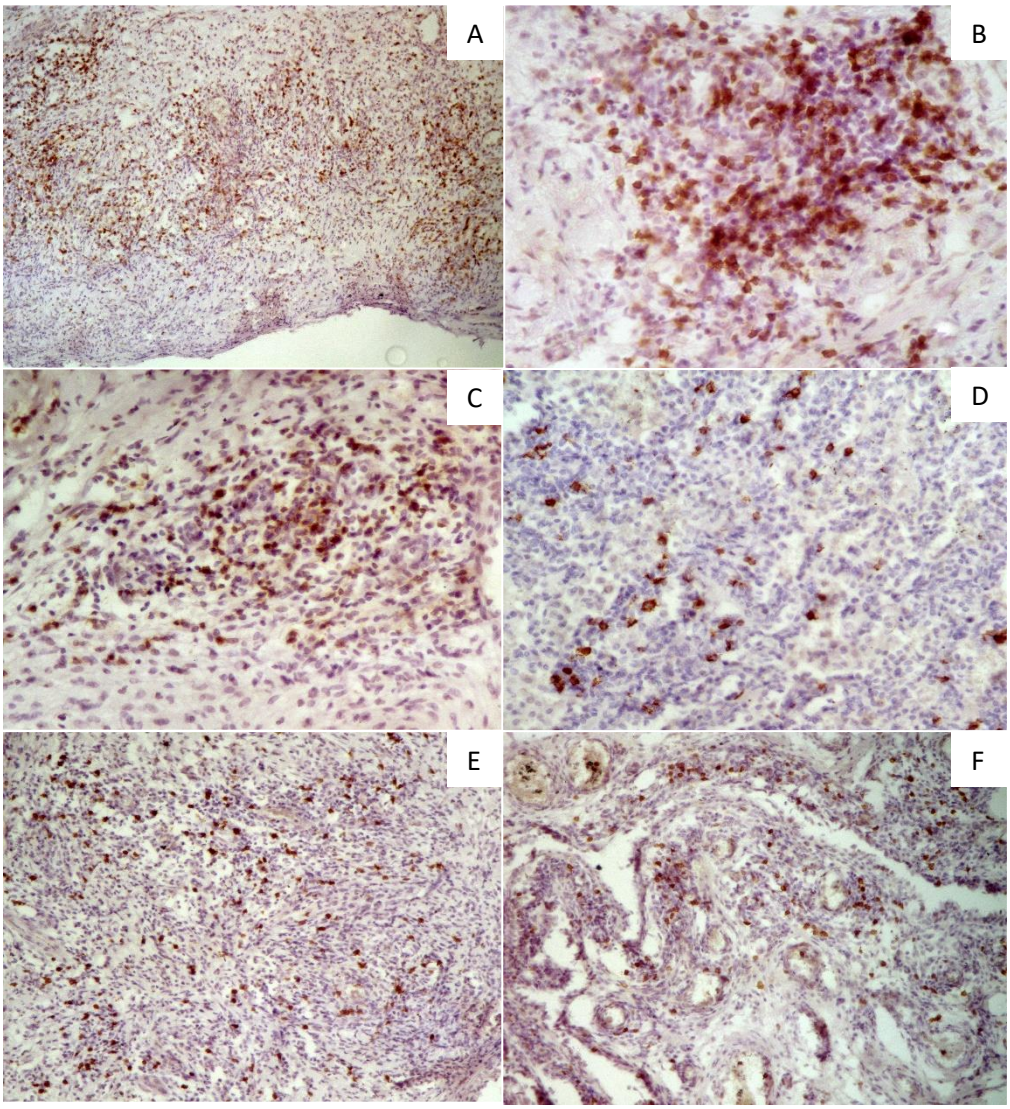

Fig. 1. Distribution of T lymphocytes in the fibrous capsule and adjacent parenchyma in study group 1: A - identification of CD3 lymphocytes in the inflammatory infiltrate of the pulmonary parenchyma underlying the capsule with recent necrolytic changes; B - perivascular inflammatory infiltrate of the pulmonary parenchyma underlying the capsule (explanations in the text); C, D - immunohistochemical identification of CD4 cells in the pulmonary parenchyma underlying the capsule (explanations in the text); E - identification of CD8 lymphocytes in the inflammatory infiltrate of the pulmonary parenchyma underlying the capsule and within the pleura (F). *Immunoreaction with anti-CD8*

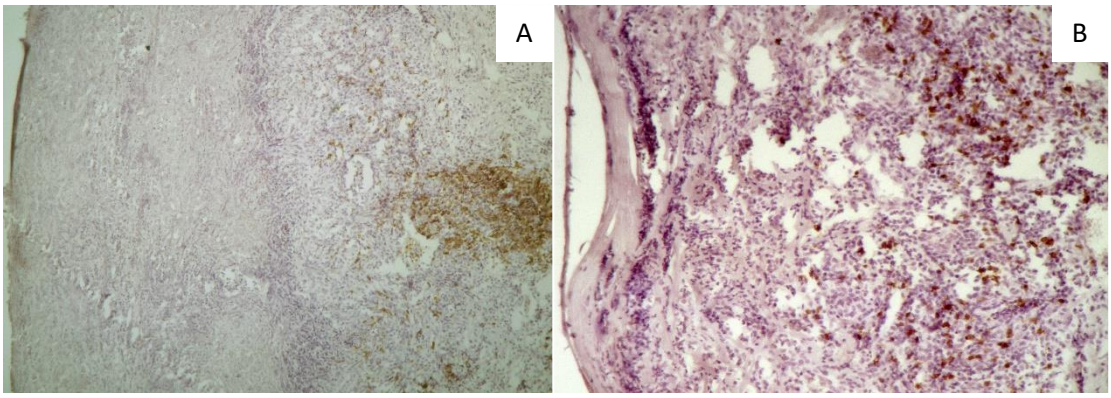

Fig. 2. Distribution of $CD20^+$ B lymphocytes in the adjacent parenchyma in study group 1. Identification of $CD20^+$ B lymphocytes in the inflammatory infiltrate of the pulmonary parenchyma underlying the capsule with recent necrolytic changes (A), and without necrolytic changes. *Immunoreaction with anti-CD20*.

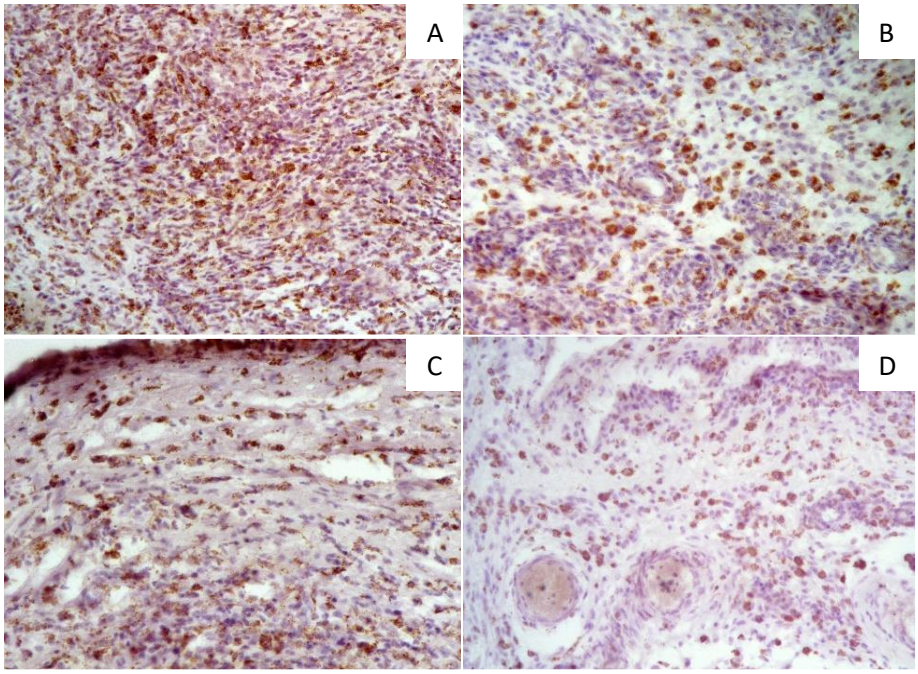

Fig. 3. . Distribution of $CD68^+$ cells in the adjacent parenchyma in study group 1: A - $CD68^+$ cells in the area of the pseudofollicular infiltrate underlying the capsule, some polynuclear cells; B - $CD68^+$ cells in the area of perivascular infiltrate with some polynucleated cells; C - $CD68^+$ cells in the area of connective capsule; D - low density $CD68^+$ cells with the presence of polynuclear cells in the pleura. *Immunoreaction with anti-CD68.*

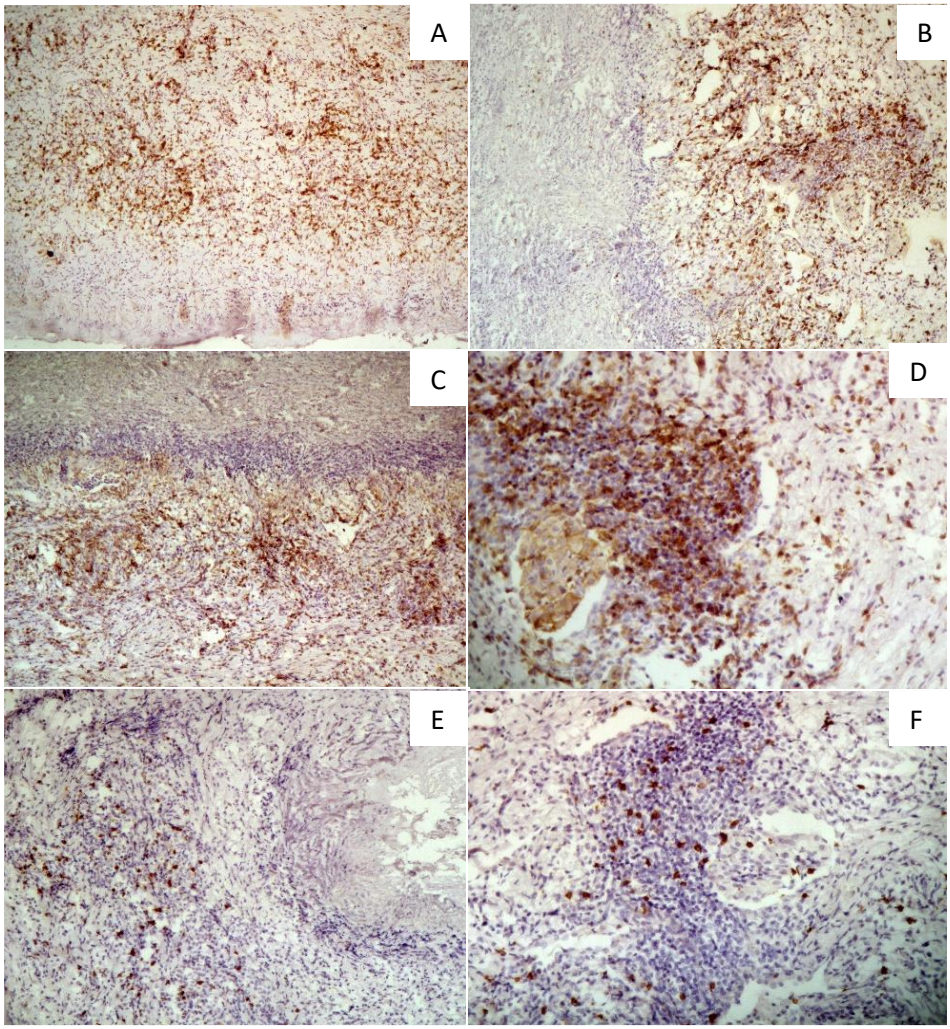

Fig. 4. The distribution of T lymphocytes in the pericystic parenchyma, group 2. A - $CD3^+$ T-lymphocytes diffusely dispersed adjacent to the capsule, solitary lymphocytes in the capsule area; B - $CD3^+$ T-lymphocytes diffusely dispersed adjacent to the capsule, peribronchially accentuated, solitary lymphocytes in the capsule area; *Immunoreaction with anti-CD3*. C - $CD4^+$ subpopulation in pseudofollicular structures in the capsule; D - $CD4^+$ subpopulation in peribronchial pseudofollicular structures; *Immunoreaction with anti-CD4*. E - subpopulation in pseudofollicular structures near the capsule with necrolytic modifications; $CD8^+$ subpopulation in peribronchial pseudofollicular structures and dispersed interstitially at distance; *Immunoreaction with anti-CD8.*

The $CD20^+$ B lymphocytes were much numerous (255.7±16.1 cells/field) compared to group 1 ($p<0.001$), being located in pericapsular inflammatory infiltrates in both dispersed and pseudofollicular aspect (fig. 5), numerous cells being observed in the fibrous capsule area.

The immunohistochemical testing of the $CD68^+$ macrophage cell component revealed that in group 2 the density of these cells (326.8±36.4 cells/field) veridically exceeded the values of group 1 ($p<0.01$). $CD68^+$ cells were predominantly concentrated in the border area between the fibrous capsule and pulmonary parenchyma, but they were found in a large number in the fibrous capsule area (fig. 6A). In the pericystic parenchyma, $CD68^+$ cells formed peribronchial pseudofollicular structures, in some places they being also observed in the bronchial lumen (fig. 6B).

In the group of patients with complicated forms of pulmonary hydatid cyst (group 3) there were increased values of CD3+ lymphocyte density (301.5±71.5 cells/field) without a statistically significant difference compared with group 1 and 2. Despite higher values, there was no real predominance of these cells in inflammatory infiltrates of the pericystic pulmonary parenchyma, these lymphocytes being unevenly spread. $CD3^+$ lymphocytes were predominantly concentrated in the sectors adjacent to the fibrous capsule, being diffusely spread in plates and dispersedly (fig. 7A). In the pericystic parenchyma, clusters of $CD3^+$ cells could be observed in peribronchial areas (fig. 7B), as well as in interalveolar septa (fig. 7C). The density of these T lymphocytes decreases while increasing the distance from the pathological focus (fig. 7D).

The density of $CD4^+$ subpopulation constituted 162.3±22.8 cells in the field of view, with no veridical difference compared to the two study groups ($p>0.05$). $CD4^+$ cells were concentrated in large inflammatory infiltrates adjacent to the fibrous capsule, being spread in plates (fig. 8A) or pseudofollicular structures (fig. 8B). Frequently, $CD4^+$ lymphocytes could be observed in the infiltrates of interalveolar septa (fig. 8C) and as interstitial follicular structures (fig. 8D).

The subpopulation of $CD8^+$ cells, estimated in group 3 (228.8±17.6 cells/field), veridically exceeded the density of these cells in group 1 ($p<0.01$) and group 2 ($p<0.05$). $CD8^+$ lymphocytes were present in areas adjacent to the fibrous capsule in the form of dispersed pseudofollicular structures (fig. 9A), as well as in peribronchial spaces (fig. 9B), these lymphocytes having a moderate density in distant areas (fig. 9C), where they could also be observed as interstitial follicular structures (fig. 9D).

The examination results of group 3 showed an insignificantly higher density of $CD20^+$ B lymphocytes (180.3±62.02 cells/field) compared to group 1 ($p>0.05$), the recorded values being lower compared to the values of group 2 with no veridical difference ($p>0.05$). These lymphocytes were observed in the form of pseudofollicular structures, located adjacent to the fibrous capsule and in the distant pulmonary parenchyma (fig. 10A), as well as peribronchially (fig. 10B).

The density of $CD68^+$ cells (201.7±47.4 cells/field) in group 3 was insignificantly higher compared to group 1 ($p>0.05$) and insignificantly lower compared to group 2 ($p>0.05$). Despite the fact that in the areas bordering with the fibrous capsule $CD68^+$ lymphocytes had a significant density (fig. 11 B), they could be observed in the adjacent parenchyma and even in the fibrous capsule (fig. 11A). There were also CD68 cells intraalveolarly and interstitially, some being polynucleated (fig, 11C).

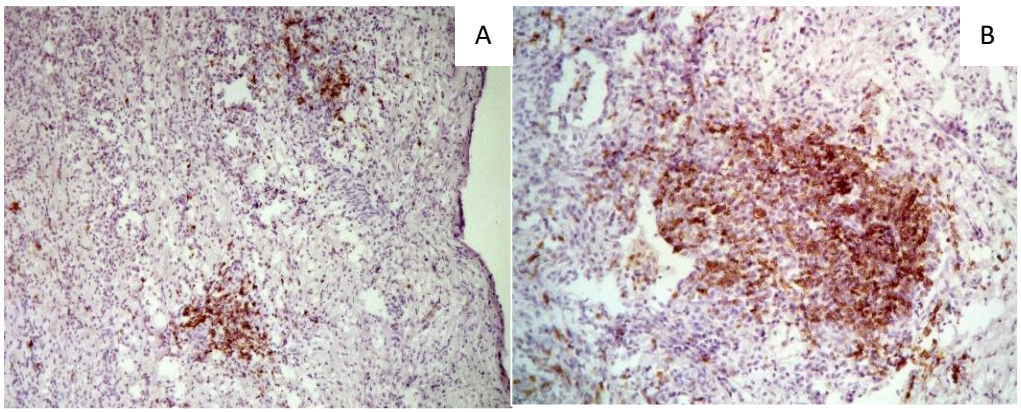

Fig. 5. Distribution of $CD20^+$ B lymphocytes in the pericystic parenchyma in group 2. A - $CD20^+$ B lymphocytes in dispersed and pseudofollicular appearance in the inflammatory infiltrate of the pulmonary parenchyma underlying the capsule with recent necrolytic changes; B - B $CD20^+$ lymphocytes in pseudofollicular structures near the capsule. *Immunoreaction with anti-CD20.*

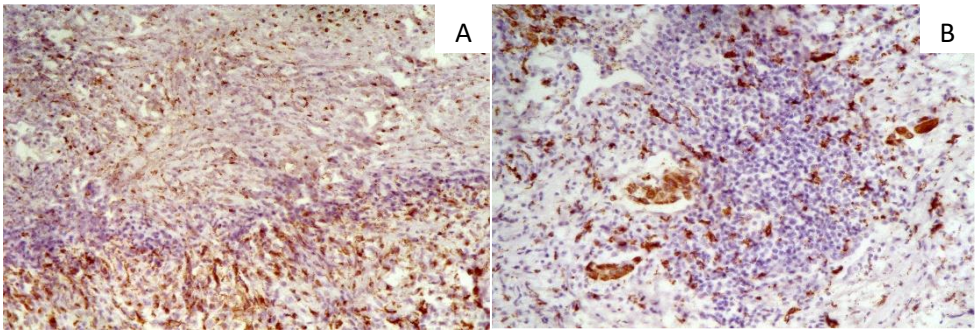

Fic. 6. Distribution of $CD68^+$ cells in the pericystic parenchyma in group 2. A - $CD68^+$ cells in the border and conjunctival capsule areas; B - $CD68^+$ cells in peribronchial pseudofollicular structures and bronchial lumen, some having polynucleated appearance. *Immunoreaction with anti-CD68*

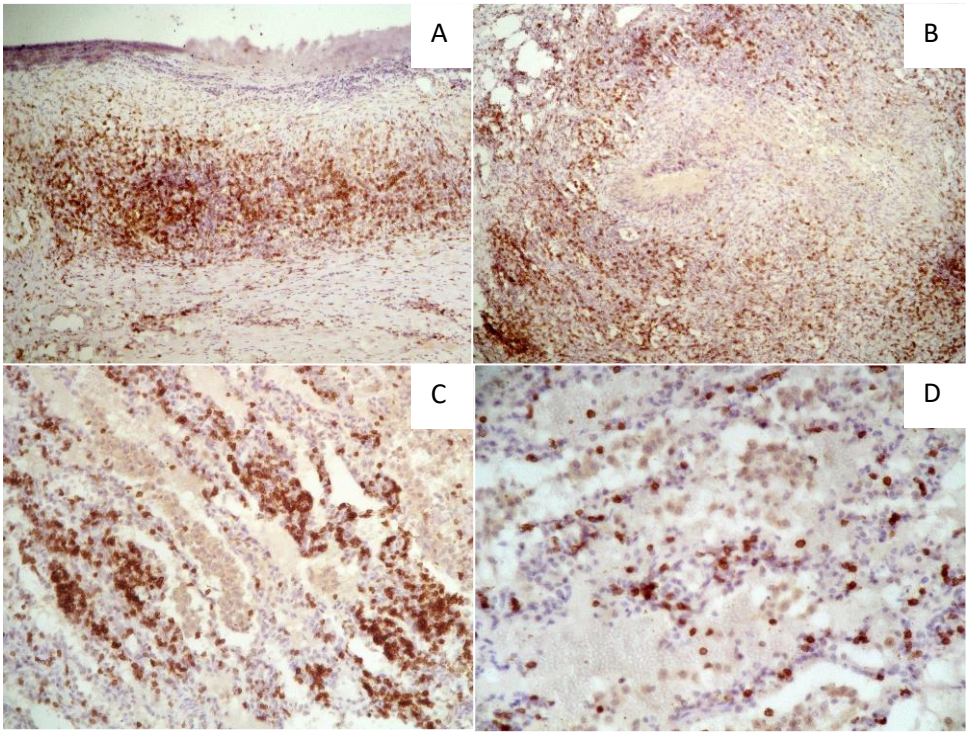

Fig. 7. Distribution of $CD3^+$ cells in the pericystic parenchyma in group 3. A - diffuse $CD3^+$ lymphocytes in plate-like and dispersed appearance adjacent to the capsule; B - peribronchially localized $CD3^+$ lymphocytes; C - $CD3^+$ lymphocytes of medium density in interalveolar septa; D - low-density $CD3^+$ lymphocytes in distant interalveolar septa; *Immunoreaction with anti-CD3.*

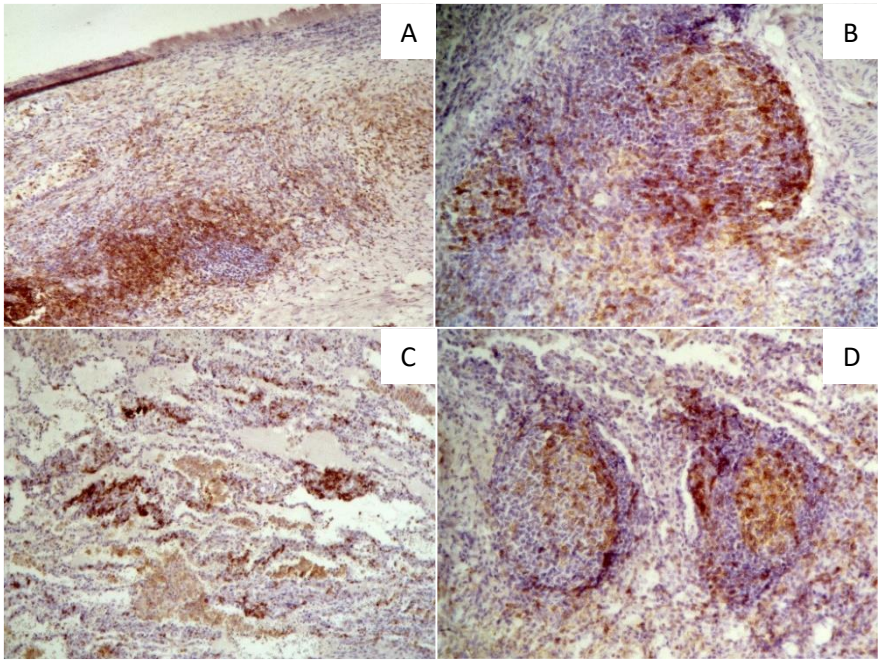

Fig. 8. Distribution of $CD4^+$ cells in the pericystic parenchyma in group 3. A - the subpopulation of $CD4^+$ in vast plate-like infiltrate around the capsule; B - $CD4^+$ lymphocytes in pseudofollicular structures around the capsule; C - $CD4^+$ lymphocytes in the infiltrate localized in interalveolar septa; D - $CD4^+$ lymphocytes in the form of interstitial follicular structures; *Immunoreaction with anti-CD4.*

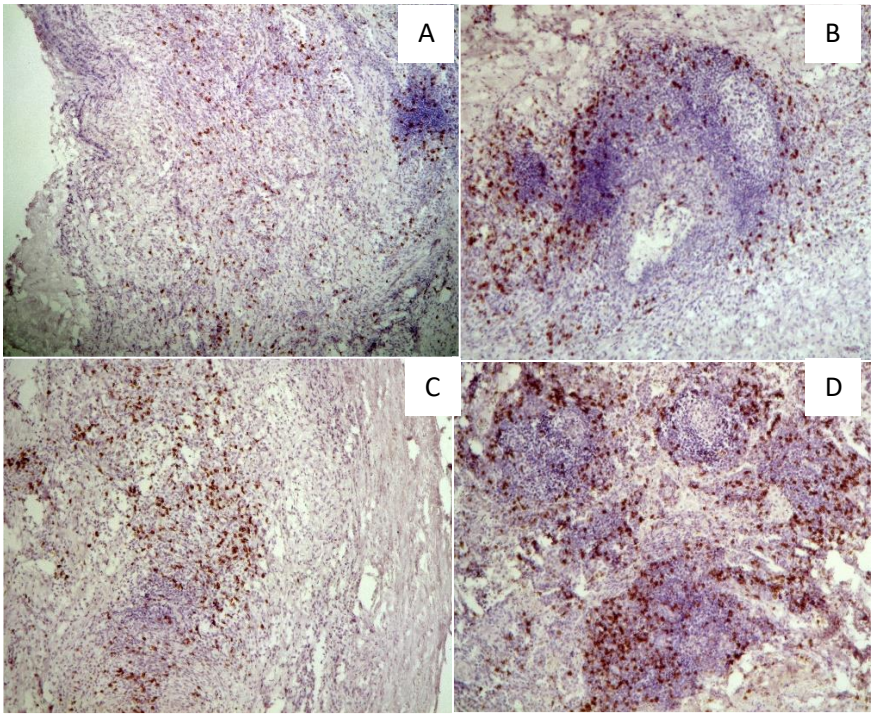

Fig. 9. Distribution of $CD8^+$ cells in the pericystic parenchyma in group 3. A - $CD8^+$ cells in pseudofollicular structures and interstitially dispersed adjacent to the capsule; B - $CD8^+$ cells in peribronchial pseudofollicular structures; C - $CD8^+$ cells of moderate density in pericapsular areas at various distance; D - $CD8^+$ cells in distant interstitial lymphoid follicular structures. *Immunoreaction with anti-CD8.*

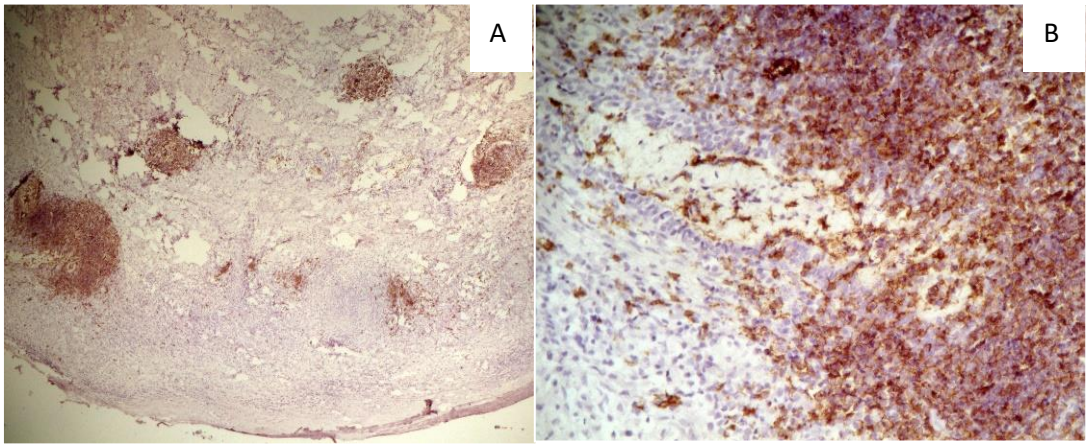

Fig. 10. Distribution of $CD20^+$ cells in the pericystic parenchyma in group 3. $CD20^+$ B lymphocytes in the form of pseudofollicular structures located around the capsule and distantly in the pulmonary parenchyma; B - $CD20^+$ B lymphocytes in peribronchial pseudofollicular structures; *Immunoreaction with anti-CD20*

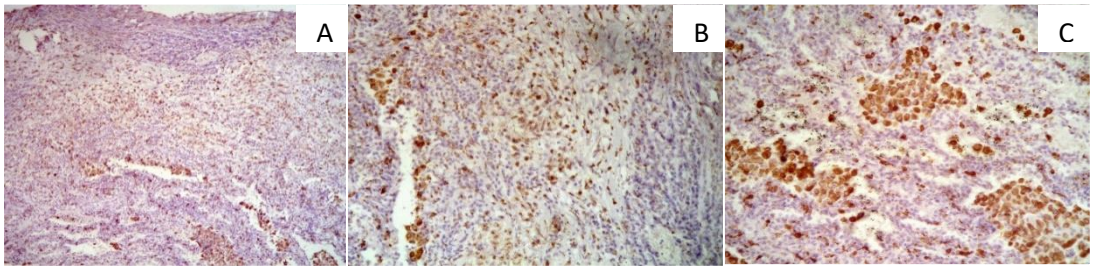

Fig. 11. Distribution of $CD68^+$ macrophages in the pericystic parenchyma in group 3. A - moderately diffuse CD68+ cells in the area of fibrous capsule and underlying parenchyma; B - $CD68^+$ cells in structures of marked density bordering with the fibrous capsule; C - $CD68^+$ cells in the intralveolar and interstitial solitary area, some polynuclear ones. *Immunoreaction with anti-CD68.*

Discussion

T lymphocytes constitute a relatively minor population in a normal lung, the number of these cells being increased, undergoing phenotypic changes in cases of the association of pulmonary inflammation and fibrosis. The role of T lymphocytes infiltrates in the development of fibrosis remains unclear, assuming that depending on the phenotypic characteristics of T lymphocytes in pulmonary infiltrates they may have a profibrotic or antifibrotic contribution [16].

Notwithstanding a significant immune response of the intermediate host [11], several mechanisms of a complex strategy have been found in the parasitic infection with Echinococcus granulosus, whereby this parasite modulates the host immune system response for long periods of time to ensure its continuous survival [8, 9]. These mechanisms can be classified into antigenic mimicry, antigenic exhaustion, antigenic variation, immunological indifference, immunological diversion, and immunological subversion [40]. It has been established that the hydatid content induces mitosis and proliferation of the subpopulations of T, B lymphocytes and macrophages [17], demonstrating a wide variety of immunomodulatory actions of the hydatid fluid, including cytotoxicity, polyclonal activation of lymphocytes T and B, influence of CD4 and CD8 cell expression, cytokine secretion, etc.[1, 14, 28, 29]. It has been found that the parasitic antigen AgB, factor EgEF-1 β/δ and other parasitic molecules have the ability to inhibit neutrophil recruitment and a number of immunomodulatory properties, inducing Th2 type of anti-inflammatory immune response, characterized by the production of IL-4, IL- 10, reduced level of IL-12 and IFN-c and IgG4 production [18, 29, 30].

Several studies have found that CD3 T lymphocytes predominate at the periphery of the hepatic hydatid cyst, followed by $CD20^+$ B lymphocytes, whereas $CD4^+$ and

$CD8^+$ cells have a weak presence around the pericyst, and the number of $CD68^+$ cells is highly variable [34]. Tissue scarring and fibrous tissue formation in chronic lesions are associated with phenotypic changes in T lymphocytes, which are involved in homeostasis disturbances of tissue. The long-lasting action of pathogen results in the differentiation of $CD4^+$ lymphocytes through which macrophages are activated with the subsequent development of fibrosis [22].

Some experimental immunohistochemical studies have highlighted the predominance of $CD8^+$ T lymphocytes at the periphery of progressive cysts [24]. It is assumed that $CD8^+$ lymphocytes are recruited to the injury site where, together with the activation of defense mechanisms, they may contribute to an increased tissue damage [40], this opinion being disputed by some authors [35].

The high density of $CD20^+$ B cells in pericystic tissue demonstrates a significant activity of the adaptive immune system, indicating the role of these cells in local immune functions against the parasite [35]. It should be taken into account that $CD4^+$ cells are essential in ensuring the microenvironment responsible for activating and differentiating B lymphocytes following exposure to antigen. It is considered that B lymphocytes located follicularly in peribronchiolar areas may contribute to the development of lymphoid tissue associated with bronchi, these cells contributing to the development of fibrosis by producing IL-6, which represents a pleiotropic cytokine, which in addition to its role in the acute phase reaction, it has various roles in the control of chronic inflammation, autoimmune processes, endothelial cell dysfunction and fibrogenesis [3, 4].

Pulmonary macrophages play a role in both acute and chronic pulmonary conditions, including cytotoxicity and fibrosis. Two phenotypically distinct subpopulations of macrophages are identified, being characterized as proinflammatory /cytotoxic M1 and M2 macrophages that participate in the regulation of inflammatory and wound repair processes, of which $CD68^+$ cells are also included [36]. M2 macrophages are also considered to be major regulators of fibrosis through the secretion of profibrotic mediators and subsequent activation of collagen-producing cells [20]. There are studies that show that $CD68^+$ cell expression testing is carried out to evaluate the inflammatory reaction in pericystic tissues of the hepatic hydatid cyst and to identify the involvement of macrophages against the parasitic agent [15, 36].

Conclusion

1. The evolution of the pulmonary hydatid cyst in children is characterized by a chronic inflammatory infiltration of the pericystic parenchyma with the predominance of CD3 T lymphocytes compared to the fibrous capsule where the necrolytic processes predominate.
2. The increased number of CD20 indicates a significant activation of the adaptive immune system in the aggravation of inflammatory processes in the pericystic parenchyma in complicated forms of the disease, the increase of the number of macrophages in these cases being insignificant.
3. The number of CD68 macrophages in the fibrous capsule and within the pleura was significantly lower compared to the density of these cells detected in inflammatory infiltrates of the pulmonary parenchyma underlying the fibrous capsule, an insignificant number being found in complicated forms of the disease.

REFERENCES

1. Ali W.R., Sadek A., Ghazi H.F. Evaluation of IL-2, IL-1 evaluation of IL-2, IL-10 and IFN-gamma immune expression in liver and spleen after treatment of experimental cystic echinococcosis.TOFIQ J. Med. Sci. 2016; 3(1):26-38.
2. Amri M., Mezioug D., Touil-Boukoffa C. Involvement of IL-10 and IL-4 in evasion strategies of Echinococcus granulosus to host immune response. Eur. Cytokine Netw. 2009; 20:63-8.
3. Atkins S.A., Turesson C., Myers J.L., Tazelaar H.D., Ryu J.H. et al. Morphologic and quantitative assessment of CD20B cell infiltrates in rheumatoid arthritis - associated nonspecific interstitial pneumonia and usual interstitial pneumonia. Arth. Rheum. 2006; 54(2):635-41.
4. Barnes T.C., Anderson M.E., Moots R.J. The many faces of interleukin-6: The role of IL-6 in inflammation, vasculopathy, and fibrosis in systemic sclerosis. HPC Int. J. Rheumatol. 2011. Art. ID 721608, 6 p. doi:10.1155/2011/721608.
5. Baz A., Ettlin G.M., Dematteis S. Complexity and function of cytokine responses in experimental infection by Echinococcus granulosus. Immunobiology. 2006; 211: 3-9.
6. Bektas S., Erdogan N.Y., Sahin G., Kir G., Adas G. Clinicopathological findings of hydatid cyst disease: A retrospective analysis. Ann. Clin. Pathol. 2016; 4(3):1071.
7. Breijo M., Anesetti G., Martinez L., Sim R.B., Ferreira A.M. Echinococcus granulosus: The establishment of the metacestode is associated with control of complement-mediated early inflammation. Exp. Parasitol. 2008; 118:188-96.
8. Cui S.J., Xu L.L., Zhang T., Xu M., Yao J. et al. Proteomic characterization of larval and adult development stages in Echinococcus granulosus reveals novel insight into host-parasite interactions. J. Proteom. 2013; 84:158-75.

9. Diaz A., Casaravilla C., Alen J.E., Sim R.B., Ferreira A.M. Understanding the laminated layer of larval Echinococcus II: immunology. Trends Parasitol. 2011; 27(6):263-72.
10. Golzari S.E.J., Sokouti M. Pericyst: The outermost layer of hydatid cyst. World J. Gastroenterol. 2014. 20(5): 1377-8.
11. Grubor N.M., Jovanova-Nesic K.D., Shoenfeld Y. Liver cystic echinococcosis and human host immune and autoimmune follow-up: A review. World J. Hepatol. 2017; 9(30):1176-89.
12. Halezeroglu S., Okur E., Tanyü O. Surgical Management for Hydatid Disease. Thorac. Surg. Clin. 2012; 22:375-85.
13. Hernandez A., O Connor J.E., Mir A. Phenotipic analysis of peripheral lymphocyte subpopulations in hydatid patients. Parasitol. Res. 1999; 85(11):948-50.
14. Kanan J.H.C., Chain B.M. Modulation od dendritic cell differention and cytokine secretion by the hydatid cyst fluid of Echinococcus granulosus. Immunology. 2006; 118:271-8.
15. Labsi M., Khelifi L., Mezioug D., Soufli I., Touil-Boukoff C. Antihydatid and immunomodulatory effects of Punica granatum peel aqueous extract in a murine model of echinococcosis. Asian Pacific J. Trop. Med. 2016; 9(3):211–20.
16. Luzina I.G., Todd N.W., Nacu N., Lockatell V., Choi J. et al. Regulation of pulmonary inflammation and fibrosis through expression of integrins V3 and V5 on pulmonary T lymphocytes. Arthritis & Rheumatism. 2009; 60(5):1530-9.
17. Macintyre A.R., Dixon J.B., Bleakley J.S., Green J.R. Echinococcus granulosus: assays for hydatid immunoregulatory factors using established lymphoid cell lines. Parasite Immunol. 2000; 22:475-85.
18. Malla N., Mewara A. Human cystic echinococcosis with special reference to India – An overview. Ann. Clin. Cytol. Pathol. 2016; 2(5):1038.
19. Monteiro K.M., de Carvalho M.O., Zaha A., Ferreira H.B. Proteomic analysis of the Echinococcus granulosus metacestode during infection of its intermediate host. Proteomics. 2010; 10:1985-99.
20. Murray P.J., Wynn T.A. Protective and pathogenic functions of macrophage subsets. Nat. Rev. Imm. 2011; 11(11):723-37.
21. Nabi M.S., Waseem T. Pulmonary hydatid disease: What is the optimal surgical strategy? Int. J. Surg. 2010. 8:612-61.
22. Pellicoro A., Ramachandran P., Iredale J.P., Fallowfield J.A. Liver fibrosis and repair: immune regulation of wound healing in a solid organ. Nat. Rev. Immunol. 2014; 13(3):181-94.
23. Rigano R., Buttari B., De Falco E., Profumo E., Ortona E. et al. Echinococcus granulosus-specific T-cell lines derived from patients at various clinical stages of cystic echinococcosis. Parasite Immunol. 2004; 26(1):45-52.
24. Sakamoto T., Cabrera P.A. Immunohistochemical observations on cellular response in unilocular hydatid lesions and lymp nodes of cattle. Acta Trop. 2003; 85(2):271-9.
25. Sarkar M., Pathania R., Jhobta A., Thakur B.R., Chopra R. Cystic pulmonary hydatidosis. Lung India. 2016; 33:179-91.
26. Sarkar S., Roy H., Sengupta M., Sarder K., Sengupta M. Cystic echinococcosis: A neglected disease at usual and unusual locations. Trop. Parasitol. 2017; 7:51-5.
27. Siracusano A., Delunardo F., Teggi A., Ortona E. Host-parasite relationship in cystic echinococcosis an evolving story. HPC. Clin. Develop. Immunol. 2012. Art. ID 639362. 12 pag. doi:10.1155/2012/639362.
28. Siracusano A., Margutti P., Delunardo F., Profumo E., Rigano R. et al. Molecular cross-talk in host-parasite relationships: The intriguing immunomodulatory role of Echinococcus antigen B in cystic echinococcosis. Int. J. Parasitol. 2008; 38:1371.
29. Siracusano A., Rigano R., Ortona E., Profumo E., Margutti P. et al. Immunomodulatory mechanisms during Echinococcus granulosus infection. Exp. Parasitol. 2008; 119:483-9.
30. SiracusanoA., Delunardo F., Teggi A., Ortona E. Cystic echinococcosis: Aspects of immune response, immunopathogenesis and immune evasion from the human host. Endocri., Metab.immune Dis. Drug Targets. 2012; 12:16-23.
31. Türkoğlu E., Demirtürk N., Tünay H., Akıcı M., Öz G., Embleton D.B. Evaluation of patients with cystic echinococcosis. Turkiye Parazitol. Derg. 2017; 41:28-33.
32. Vatankhah A., Halász J., Piurkó V., Barbai T., Rásó E., Tímár J. Characterization of the inflammatory cell infiltrate and expression of costimulatory molecules in chronic echinococcus granulosus infection of the human liver. BMC Inf. Dis. 2015; 15:530. DOI 10.1186/s12879-015-1252-x.
33. Vatankhan A. Immunopathology of hydatid infection in human liver. PhD Thesis. Budapest. 2016. 139 p.
34. Venosa A., Malaviya R., Choi H., Gow A.J., Laskin J.D., Laskin D.L. Characterization of distinct macrophage subpopulations during nitrogen mustard-inuced lung injury and fibrosis. Am. J. Respir. Cell Mol. Biol. 2016; 54(3):436-46.
35. Virginio V.G., Monteiroa K.M. Drumond F., de Carvalhoa M.O., Vargas D.M. et al. Excretory/secretory products from in vitro-cultured Echinococcus granulosus protoscoleces. Mol. Biochem. Parasitol. 2012; 183:15-22.
36. Vismarra A., Mangia C., Passeri B., Brundu D., Masala G. et al. Immuno-histochemical study of ovine cystic echinococcosis (Echinococcus granulosus) shows predominant T cell infiltration in established cysts. Vet. Parasitol. 2015. 209:285-8.
37. Wei X., Xu Q., Rexiti F.L., Zhu M., Lin R., Wen H. Dynamic changes of DC ant T cell subsets in mice during Echinococcus multilocularis infection. Cent. Eur. J. Immunol. 2014; 39(1):19-24.
38. Weiskirchen R., Tacke F. Cellular and molecular functions of hepatic stellate cells in inflammatory responces and liver immunology. Hepatobiliary Surg. Nutr. 2014; 3(6):344-63.
39. Zhang W., Ross A.G., McManus D.P. Mechanisms of immunity in hydatid disease: Implications for vaccine development. J. Immunol. 2008; 181:6679-85.
40. Zhang W., Wen H., Li J., Lin R., McManus D.P. Immunology and immunodiagnosis of cystic echinococcosis: An update. HPC Clin. Develop. Immunol. 2012. Art. ID 101895. 10 p. doi:10.1155/2012/101895.